# Observation of an Energetic-Particle-Driven Instability in the Wall-Stabilized High-$\beta$ Plasmas in the JT-60U Tokamak

G. Matsunaga, N. Aiba, K. Shinohara, Y. Sakamoto, A. Isayama, M. Takechi, T. Suzuki, N. Oyama, N. Asakura, Y. Kamada, T. Ozeki, and JT-60 Team

*Japan Atomic Energy Agency, Naka 311-0193, Japan*

(Received 8 January 2009; published 21 July 2009)

We have observed a bursting mode in the high-$\beta$ plasmas above the ideal $\beta$ limit without a conducting wall. The mode frequency is chirping down as the mode amplitude increases, and its initial value is close to the precession frequency of the trapped energetic particle from the perpendicular neutral beams. The mode structure is radially extended with a peak around the $q = 2$ surface. This mode can finally trigger the resistive wall mode (RWM) despite enough plasma rotation for RWM stabilization. It is concluded that the mode is driven by trapped energetic particles. The mode is attributed to the interaction between the trapped energetic particles and a marginally stable mode in the wall-stabilized high-$\beta_N$ region.

DOI: 10.1103/PhysRevLett.103.045001 PACS numbers: 52.35.Py, 52.55.Fa, 52.55.Tn

Toward a nuclear fusion reactor, operations in the high-$\beta$ (the ratio of plasma pressure to magnetic field pressure) region are desirable from an economical point of view because the fusion output is proportional to the square of $\beta$. However, according to the ideal MHD theory, the achievable $\beta$ is determined by the stability of ideal kink-ballooning modes (IKBMs) with a low toroidal mode number $n$. The IKBM can be stabilized by a perfectly conducting wall (ideal wall) close to the plasma boundary. Therefore, the ideal wall makes it possible to increase achievable $\beta$ in the high-$\beta$ region $\beta_N^{\mathrm{free}} \leq \beta_N \leq \beta_N^{\mathrm{ideal}}$, that is called as the wall-stabilized high-$\beta$ region. Here, $\beta_N^{\mathrm{free}}$ and $\beta_N^{\mathrm{ideal}}$ are the ideal $\beta$ limits without and with the ideal wall and $\beta_N$ is the so-called ''normalized $\beta$'' or ''Troyon $\beta$'' defined as $\beta_N = \beta[\%]a[\mathrm{m}]/(I_p[\mathrm{MA}]B_T[\mathrm{T}])$, where $a$, $I_p$, and $B_T$ are a plasma minor radius, the plasma current, and the toroidal magnetic field, respectively [1]. In actual devices that have a conducting wall with a finite resistivity, the resistive wall mode (RWM), whose growth time corresponds to the current diffusion time in a resistive wall, appears as another mode so as to limit achievable $\beta$ in the wall-stabilized high-$\beta$ region. With respect to the RWM stabilization, the plasma rotation effect is theoretically predicted with several dissipations [2–5]. Moreover, recent experiments have shown that the required rotation for the RWM stabilization is less than about 1% of Alfvén velocity $V_A$ at the rational surface [6–8]. Recently, to explain this slow critical rotation for RWM stabilization, kinetic contributions of bulk plasma and energetic particles are considered to be important [9,10], and are being investigated experimentally.

In this Letter, we report a newly observed bursting mode in the high-$\beta$ plasmas on the JT-60U tokamak device. The bursting mode behaves like the so-called ''fishbone'' [11] and has a growth time with a few milliseconds accompanied by frequency chirping down. The initial mode frequency is close to the precession frequency of the trapped particle from the neutral beams injected perpendicular to $B_t$ (PERP-NB), suggesting that the mode is driven by trapped energetic particles. The mode has been observed only in the wall-stabilized high-$\beta$ region where the IKBM and RWM are marginally stable, which are stabilized by the conducting wall and the plasma rotation, respectively. The mode structure is radially extended, which is quite similar to those of these stable MHD modes. The mode can finally trigger the RWM despite enough plasma rotation for RWM stabilization. For these experimental results, we conclude that this bursting mode is attributed to the interaction between the kinetic contribution of energetic particles and a marginally stable mode that exists in the wall-stabilized high-$\beta$ region. Therefore, we have named this mode the ''energetic-particle-driven wall mode (EWM).''

The observed fishbone-like burst mode, hereafter called the ''EWM,'' has a very large amplitude up to 1 G detected by the toroidal saddle loops at the wall. Typical waveforms of the EWM are shown in Fig. 1(a) as the magnetic fluctuation measured by the toroidal saddle loops. These are Fourier-decomposed fluctuations as the toroidal mode number $n = 1$. Usually, the growth time of the mode is about $\tau_g \sim 1$ ms. Note that the parameters of the discharges shown in this Letter are as follows: $I_p = 0.9$ MA, $B_t = 1.5$–$1.7$ T, the line-averaged electron density $\bar{n}_e \simeq 3 \times 10^{19}$ m$^{-3}$, and the normalized wall radius $d/a \leq 1.25$. The EWM sometimes directly induces the RWM onset despite the plasma rotation larger than a critical rotation for RWM stabilization. For example, the first EWM directly induced the $n = 1$ RWM as shown in Fig. 1(a) and 1(b). The radial displacement, and thus eigenmode structure, is estimated by $\delta T_e/\nabla T_e$ from the electron cyclotron emission (ECE) system [12]. In Fig. 1(c), the eigenmode structure and the profile of the safety factor $q$ measured with the motional stark effect (MSE) system [13] are plotted. It shows that the EWM has a radially extended eigenfunction with a peak around the $q = 2$ at $r/a \simeq 0.6$.

 

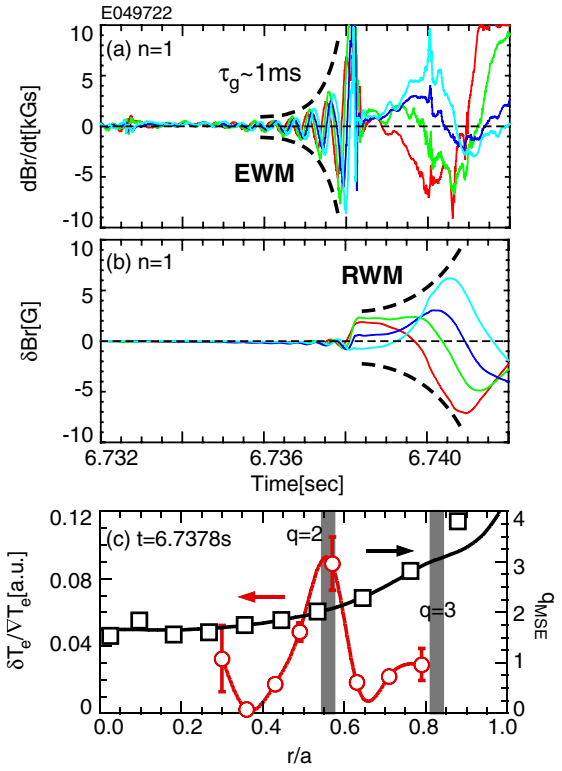


FIG. 1 (color online). Typical waveforms of EWM: (a) $n = 1$ magnetic fluctuations measured by the toroidal saddle loops, and (b) integrated ones. Different colors correspond to the saddle loops at the different toroidal locations. (c) Profiles of the radial displacement and safety factor obtained by ECE and MSE measurements.

By the toroidally located eight saddle loops, the toroidal mode number is clearly $n = 1$. By the poloidally distributed magnetic probes, the poloidal one seems to be $m = 3$–$4$ at the wall, and the mode amplitude at the low-field side is much larger than at the high-field side; thus, the mode has a ballooning structure.

Figures 2(a) and 2(b) show the EWM mode amplitude and frequency with the plasma toroidal rotation frequency at $q \simeq 2$ measured by the fast-charge exchange recombination spectroscopy (CXRS) with a sampling rate of 400 Hz [14]. The mode frequency, whose initial frequency is about 3 kHz, is chirping down as the amplitude is increasing. And the mode is often accompanied by the $D_\alpha$ spike due to the edge localized mode. The mode is always propagating in the co-current direction toroidally and in the ion diamagnetic $\omega_*^i$ direction poloidally even though the plasma is rotating in the counter-current direction as shown in Fig. 2(c). This means that the EWM frequency does not correspond to the plasma rotation anywhere.

The initial mode frequency is close to the precession frequency of the trapped energetic particle, suggesting that the EWM is driven by trapped energetic particles. To clarify the driving force of the EWM, the PERP-NB power was switched on or off before and during the EWM as shown in Fig. 3 with neutron emission $S_n$. After one of the

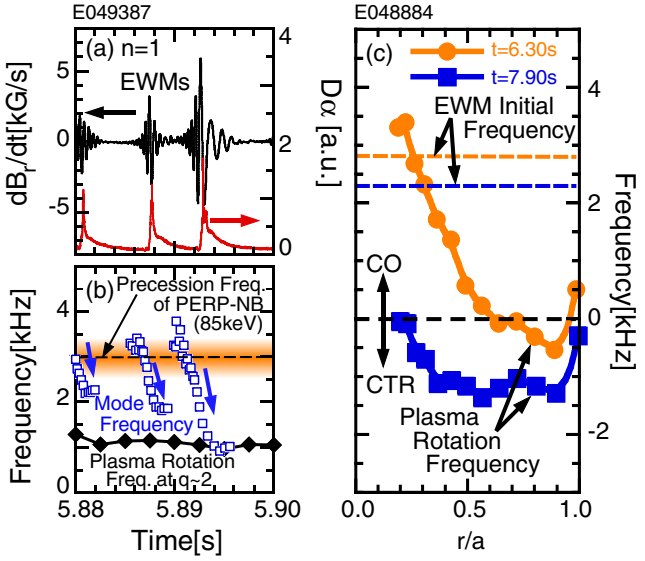


FIG. 2 (color online). Waveforms of (a) EWM amplitude and $D_\alpha$ emission, (b) mode frequency with the plasma rotation frequency at $q \simeq 2$. (c) Comparison of plasma rotation profiles measured by CXRS with EWM initial frequency.

PERP-NBs was switched on, EWM mode amplitude was gradually increasing with increasing $S_n$. While just after the PERP-NB was switched off, the EWM quickly decayed within their slowing down time $\tau_{sd} \sim 0.1$ s. It should be noted that $\beta_N$ was almost constant even though the NB power was reduced. This suggests that the EWM is attributed to energetic particles with $E_b = 85$ keV just after the ionization. These results support the interpretation that the EWM is driven by the trapped energetic particles of the PERP-NBs.

We have shown that the injection of PERP-NBs is one of the "necessary conditions" for the EWM and now we

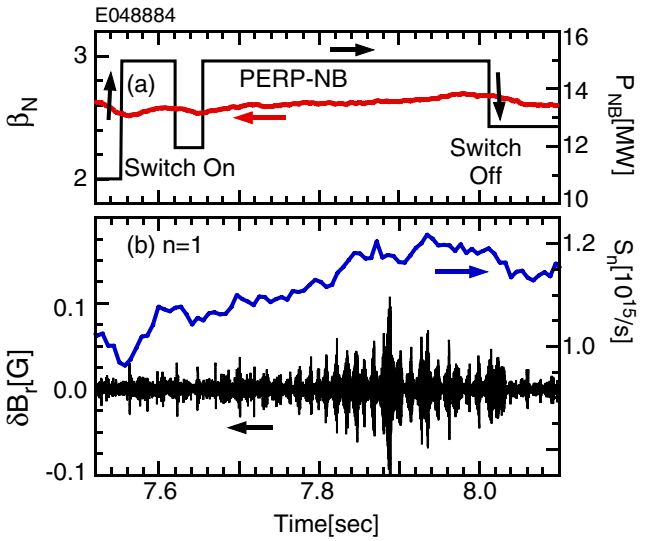


FIG. 3 (color online). Waveforms of NB power switch on/off discharge: (a) temporal evolution of $\beta_N$ and NB power, and (b) integrated $n = 1$ magnetic fluctuation and neutron emission.

demonstrate that $C_\beta \geq 0$ is also required, where $C_\beta$ is defined as $C_\beta = (\beta_N - \beta_N^{\rm free})/(\beta_N^{\rm ideal} - \beta_N^{\rm free})$, namely $C_\beta = 0$ and 1 correspond to the no-wall ($\beta_N = \beta_N^{\rm free}$) and ideal wall ($\beta_N = \beta_N^{\rm ideal}$) limits, respectively. Figure 4 shows the three discharges comparing different $C_\beta$ and $\beta_N$. These $C_\beta$ and $\beta_N$ were changed by the NB power and its injection timing. Since the delayed NB injection allows the plasma current penetration, the internal inductance $l_i$ increased. The no-wall $\beta_N$ limit tends to be proportional to $l_i$ [15]. Actually, for these discharges, the ideal and no-wall $\beta_N$ limits are estimated as $\beta_N^{\rm ideal} \sim 4l_i$ and $\beta_N^{\rm free} \sim 3l_i$ by the stability analysis using MARG2D [16], respectively. In Figs. 4(a) and 4(b), where $C_\beta > 0$ with different $\beta_N$, the EWMs have been observed. In these discharges, the main NB heating was carried out at the beginning of the $I_p$ flat top after the preheating during the $I_p$ ramp to keep a weak magnetic shear. The plasma supported by early NB injection gives low $\beta_N^{\rm free} \sim 2.4$ due to lower $l_i$. Finally, these discharges were terminated by the $n = 1$ RWMs triggered by the EWMs. On the other hand, as shown in Fig. 4(c), the main NB heating was delayed to increase $\beta_N^{\rm free}$ up to 3. In this discharge, the EWM was not observed despite $\beta_N \sim$ 3.0 and full PERP-NB injections.

The EWM waveforms are quite similar to the so-called fishbone instability associated with an $m/n = 1/1$ internal kink mode as the center value of safety factor $q_0$ is close to or below unity. The fishbone instability is well documented experimentally and theoretically in Refs. [11,17–21]. The fishbone instability can be destabilized by the kinetic contribution of the energetic particles near the marginal stability of the $m/n = 1/1$ internal kink mode. While, in these discharges where the EWMs were observed, $q_0$ is not close to unity but $q_0 = 1.6 \pm 0.4$ as shown in Fig. 1(c). This means that an $m/n = 1/1$ internal kink mode is fairly stable in these discharges, that is, it is concluded that the observed mode is not originated from the $m/n = 1/1$ internal kink mode. On the other hand, the mode is observed only in the wall-stabilized high-$\beta$ region $C_\beta \geq 0$. In this region, the IKBM and RWM are predicted to be marginally stable due to the wall and/or plasma rotation stabilization effects. On the analogy of $m/n = 1/1$ fishbones, the EWM is considered to be caused by the kinetic contribution of the energetic particles and either of the marginally stable modes.

For validation of the hypothesis that the EWM can be destabilized in the wall-stabilized region $C_\beta \geq 0$, the stability domains are statistically plotted in Fig. 5. First, the $\beta_N$ vs $l_i$ region is shown in Fig. 5(a) with the ideal and no-wall $\beta_N$ limits as the dashed lines. The data points correspond to each EWM burst, and triangles are the data of the discharges in Fig. 4. As seen in Fig. 5(a), the EWM is only observed in the $C_\beta \geq 0$ region, that is, $C_\beta \geq 0$ is one of "necessary conditions" for the EWM destabilization. Second, the EWM mode amplitude on the $P_{\rm NB}^{\rm perp}/P_{\rm NB}^{\rm total}$ region is shown in Fig. 5(b). The amplitude tends to be larger as $P_{\rm NB}^{\rm perp}/P_{\rm NB}^{\rm total}$ is increased. This suggests that the trapped energetic particle is the driving source for the EWM. Third, Fig. 5(c) shows $\beta_N/l_i$ vs the absolute value of $V_{\rm tor}$ around the $q = 2$ surface with a $V_{\rm tor}/V_A$ scale. As the plasma rotation is increased, the boundary for the EWM observation also increases. This trend qualitatively suggests the rotation stabilizing effect. From these results, since the observed fishbone-like instability EWM is driven by the trapped energetic particles in the wall-stabilized high-$\beta$ region.

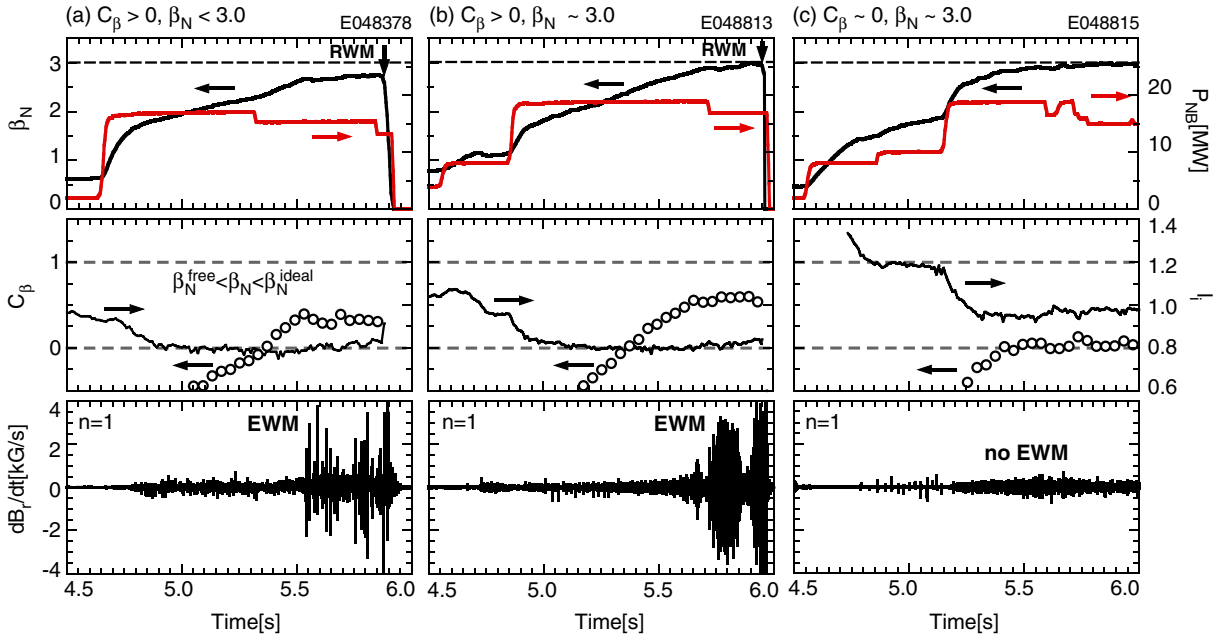


FIG. 4 (color online). Comparison of three discharges with different $\beta_N$ and $C_\beta$. From the top, $\beta_N$ and NB power, internal inductance $l_i$ and $C_\beta$, and the $n = 1$ magnetic fluctuation. From the left, $(C_\beta, \beta_N) \simeq (0.4, 2.7)$, (0.6, 3.0), and (0.0, 3.0).

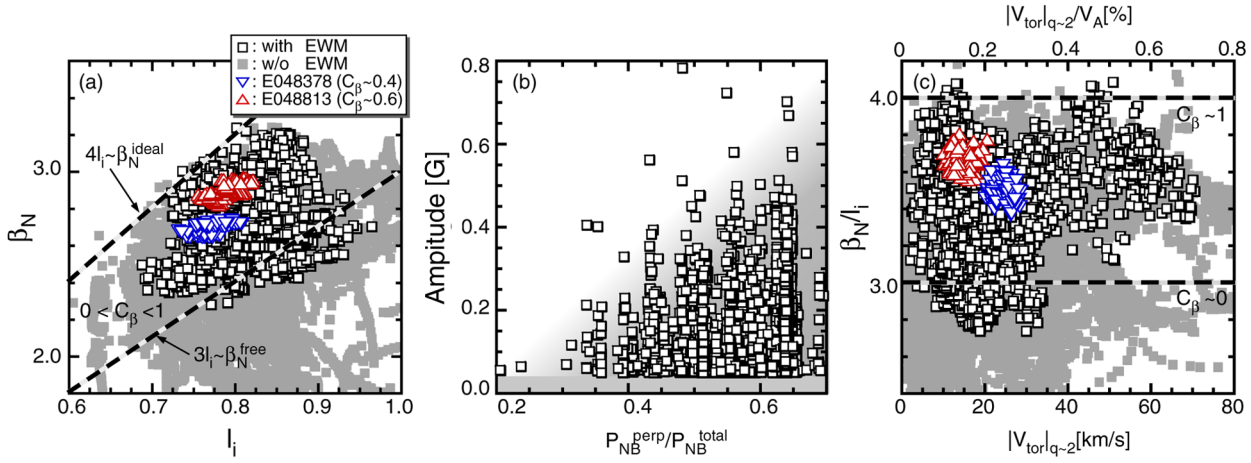


FIG. 5 (color online). EWM stability domains as (a) $\beta_N$ vs $l_i$, (b) EWM amplitude vs $P_{\mathrm{NB}}^{\mathrm{perp}}/P_{\mathrm{NB}}^{\mathrm{total}}$, and (c) $\beta_N/l_i$ vs $|V_{\mathrm{tor}}|_{q\sim2}$ regions. The dashed lines are the ideal and no-wall $\beta_N$ limits estimated by MARG2D as $\beta_N^{\mathrm{ideal}} \sim 4l_i$ and $\beta_N^{\mathrm{free}} \sim 3l_i$, respectively. Triangles are the data of the discharges in Figs. 4(a) and 4(c).

In conclusion, we have newly observed a fishbone-like instability EWM in the wall-stabilized high-$\beta$ plasmas where the IKBM and RWM are predicted to be marginally stable by the wall and/or plasma rotation stabilizing effects. This mode can directly trigger the RWM despite enough plasma rotation for RWM stabilization. The radial mode structure is globally extended around the $q = 2$ surface, which is quite similar to the $n = 1$ IKBM and RWM. The mode frequency is close to the precession frequency of the trapped energetic particles from the perpendicular neutral beams. This mode can be stabilized by reducing the PERP-NBs while keeping $\beta_N$, indicating that the mode is driven by trapped energetic particles. Moreover, the mode is observed only in the wall-stabilized high-$\beta$ plasma $C_\beta \geq 0$. These means that both the trapped energetic particle pressure and $C_\beta \geq 0$ are "necessary conditions" for the EWM destabilization. Based on these experimental observations, it is concluded that this mode is driven by the kinetic contribution of energetic particles. Namely, this mode is considered to be the energetic particle branch with taking into account the kinetic contribution of the energetic particles in the dispersion relation for the wall-stabilized high-$\beta$ plasma. We have named this mode as EWM. This situation is very similar to the so-called fishbone instability associated with the $m/n = 1/1$ internal kink mode. In analogy with the fishbone and the sawtooth stabilization by energetic particles [19], the IKBM and/or RWM could be stabilized by the energetic particle. In particular, since $\alpha$-particle contribution to the MHD stability is predicted in ITER and fusion reactors, a special attention should be paid to high-$\beta$ operation above $\beta_N^{\mathrm{free}}$ where the IKBM and RWM are predicted to be marginally stable. For validation of these points, further theoretical work is required.

One of the authors, G. M., would like to thank Dr. M. Okabayashi (PPPL) and Professors K. Toi (NIFS) and Y. Todo (NIFS) for several useful discussion. This work was supported in part by a Grant-in-Aid for Young Scientists (B) from the Ministry of Education, Culture, Sports, Science, and Technology of Japan, No. 21760702.

[1] F. Toroyon *et al.*, Plasma Phys. Controlled Fusion **26**, 209 (1984).
[2] A. Bondeson and D. J. Ward, Phys. Rev. Lett. **72**, 2709 (1994).
[3] M. S. Chu *et al.*, Phys. Plasmas **2**, 2236 (1995).
[4] R. Fitzpatrick and A. Y. Aydemir, Nucl. Fusion **36**, 11 (1996).
[5] R. Betti and J. P. Freidberg, Phys. Rev. Lett. **74**, 2949 (1995).
[6] G. Matsunaga *et al.*, in *Proceedings of the 33rd EPS Conference on Plasma Physics* (Rome, Italy, 2006), CD-ROM (File No. O2.003).
[7] M. Takechi *et al.*, Phys. Rev. Lett. **98**, 055002 (2007).
[8] H. Reimerdes *et al.*, Phys. Rev. Lett. **98**, 055001 (2007).
[9] B. Hu and R. Betti, Phys. Rev. Lett. **93**, 105002 (2004).
[10] P. Lauber and S. Günter, Nucl. Fusion **48**, 084002 (2008).
[11] K. McGuire *et al.*, Phys. Rev. Lett. **50**, 891 (1983).
[12] N. Isei *et al.*, Rev. Sci. Instrum. **66**, 413 (1995).
[13] T. Fujita *et al.*, Fusion Eng. Des. **34–35**, 289 (1997).
[14] K. Ida *et al.*, Rev. Sci. Instrum. **79**, 053506 (2008).
[15] W. Howl *et al.*, Phys. Fluids B **4**, 1724 (1992).
[16] S. Tokuda and T. Watanabe, Phys. Plasmas **6**, 3012 (1999).
[17] L. Chen *et al.*, Phys. Rev. Lett. **52**, 1122 (1984).
[18] B. Coppi and F. Porcelli, Phys. Rev. Lett. **57**, 2272 (1986).
[19] F. Porcelli, Plasma Phys. Controlled Fusion **33**, 1601 (1991).
[20] R. Betti and J. P. Freidberg, Phys. Rev. Lett. **70**, 3428 (1993).
[21] W. W. Heidbrink *et al.*, Phys. Rev. Lett. **57**, 835 (1986).